

Performance of a phased array for ^{31}P cardiac MR spectroscopy

C. T. Rodgers¹, L. E. Cochlin², D. J. Tyler², S. Neubauer¹, and M. D. Robson¹

¹Oxford Centre for Clinical Magnetic Resonance Research, University of Oxford, Oxford, United Kingdom, ²Department of Physiology, Anatomy and Genetics, University of Oxford, United Kingdom

Cardiac ^{31}P magnetic resonance (MR) spectra of high-energy phosphorus metabolites are typically acquired using a transmit/receive (Tx/Rx) surface coil. In MR imaging, single element surface coils have largely been superseded by receive arrays, which provide higher signal-to-noise ratios (SNRs) and larger fields of view (FOVs). We present results from an 8-element cardiac ^{31}P receive array, used to measure the first receive array cardiac ^{31}P spectra at 3T. We benchmark these spectra against an established protocol¹ in 8 normal volunteers.

Methods: Cardiac ^{31}P MR spectra were recorded from normal volunteers (N=8, 28-42 years, 7m) in a 3T Trio MRI scanner (Siemens) with a ^{31}P array (Rapid Biomedical) comprising anterior (30×29cm Tx and 4 20×6cm Rx elements) and posterior portions (4 20×6cm Rx elements). The standard Siemens ^1H body coil was used for imaging and B_0 shimming. Cardiac ^{31}P spectra were acquired using a UTE-CSI pulse sequence¹, ECG gating and a 35×35×35cm FOV large enough to prevent wrap artefacts. B_1 was calibrated with a 2.5mL K_2HPO_4 phantom to give the Ernst flip angle for PCr in the heart (at 12cm²). A CSI matrix of 22×22×10 voxels and 2 averages were used with acquisition weighting³. Control spectra were recorded using an established optimized protocol¹ with a standard $^{31}\text{P}/^1\text{H}$ 1.5T Siemens heart/liver coil (26×28cm $^{31}\text{P}/^1\text{H}$ Tx and a loop/butterfly Rx [12×15cm and 23×12cm]) adapted for use at 3T. Control spectra used the same UTE-CSI sequence, with a 16×16×8 matrix, 24×24×20cm FOV and 10 averages to give an equal point spread voxel volume and total acquisition time. Volunteers lay supine with the array and prone with the control coil. For each subject, corresponding sets of three voxels from the centre and front of the ventricular septum in the CSI slice that passes through the papillary muscles were selected without reference to the measured spectra. Data from the array were combined using the WSVD algorithm⁴ to give a single spectrum per voxel. Control spectra were corrected for coil loading and position in Matlab. Then 11 peaks were fitted (PCr, ATP, PDE and 2,3-DPG) using AMARES. The fitted amplitudes were corrected for saturation effects and blood contamination using data from the literature.

Results: Fig. 1 shows an illustrative spectrum from the array coil. The spectral SNR was measured as the ratio of the peak amplitude of the fitted PCr peak to the baseline standard deviation. Averaging for all subjects the three voxels from the centre and front of the heart, where both coils detect ^{31}P spectra, the measured SNR is 9.2 for the array and 9.8 for the control coil (a difference of 6%). However, the standard deviation in SNR is 4.5 for the array and 6.4 for the control coil. Thus, the two coils demonstrate comparable performance for the centre and front of the heart, but the array coil gives more consistent SNR. After correcting the fitted amplitudes for saturation, NOE (for the control coil) and blood contamination using established procedures¹, the uncertainties in the final estimated PCr/ATP ratios were 16.1% for the control coil and 18.6% for the array.

Fig. 2 plots the amplitude of the β -ATP and PCr signals for each voxel in one CSI slice. Strong β -ATP signals are observed from liver and heart. PCr is detected at high levels in skeletal muscle and heart. These metabolite maps demonstrate the large FOV of the array, which detects signals throughout the volunteer's torso (23cm depth), whilst the control coil only detects signals up to \approx 13cm depth and also has a smaller lateral FOV.

Discussion: The earliest cardiac ^{31}P array increased the SNR \approx 30% and increased the FOV compared to a single element coil⁵. We observed a similar enhancement of the FOV and uniformity, as evidenced by Fig. 2. This made coil positioning less critical, reducing the standard deviation of SNR between measurements. This is the first cardiac ^{31}P array to contain posterior elements⁵. In the three voxels from one subject, the posterior elements contributed 15-22% of the signal, increasing to 35% for a voxel at the posterior ventricle wall. Indeed, it was barely possible to discern any spectrum there from the individual array elements, but the combined spectrum resembled a noisier Fig. 1. Volunteers reported that lying supine with the array was more comfortable. This has little effect on heart-coil spacing², so longer scans may be tolerable in future work.

As yet, we have not observed unequivocally the anticipated SNR advantage of the array coil compared to control experiments following currently optimal cardiac ^{31}P protocols. This is because a software limitation disallows application of NOE pulses for such surface coils. The SNR enhancement from NOE is 13-43%¹, compared to reported SNR advantages of cardiac ^{31}P array reception of \approx 30%⁵. Thus, the array coil currently equals but does not yet surpass the current optimal SNR. Given these promising results, we are pressing ahead to implement NOE enhancement. We will also implement SENSE parallel spectroscopy in order to maximise the SNR per unit time and spatial homogeneity of data from the array.

Conclusions: Phased-array ^{31}P MR spectroscopy improves SNR, FOV and homogeneity at 3T as has been previously reported at 1.5T⁵. The posterior elements introduced here contribute 35% to the signal from the posterior of the heart and provide additional information for correction of coil homogeneity. With supine positioning and the promise of greater SNR with NOE enhancement, we further advance cardiac ^{31}P methods, bringing us closer to the dream of a practical, clinical, whole heart, high-energy phosphorus metabolite exam.

References: 1. Tyler, D. J. *et al.* NMR Biomed. **22**, 405-413 (2009); 2. Schroeder, J. L. *et al.* Proc. ISMRM 3097 (2006); 3. Pohmann, R. & Kienlin, M., Magn. Reson. Med. **45**, 817-826 (2001); 4. Rodgers, C. T. & Robson, M. D., Magn. Reson. Med. In press (2009); 5. Hardy, C. J., *et al.* Magn. Reson. Med. **28**, 54-64 (1992).

Fig. 1: Spectrum from a single voxel obtained with the ^{31}P array, with no processing except zero- and first-order phase correction.

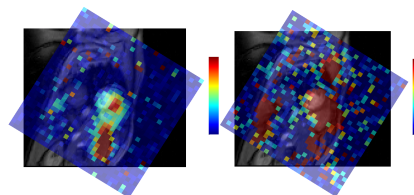
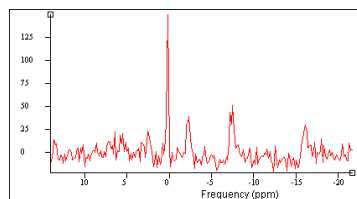


Fig. 2: Metabolite map showing fitted amplitude of (left) β -ATP and (right) PCr measured with the ^{31}P array.